Materials and Design 36 (2012) 584–589

Contents lists available at SciVerse ScienceDirect

Materials and Design

journal homepage: www.elsevier.com/locate/matdes

Evolution of the microstructure and tribological performance of Ti–6Al–4V cladding with TiN powder

Yu-Chi Lin [a], Yuan-Ching Lin [b], Yong-Chwang Chen [a,*]

[a] Department of Mechanical Engineering, National Taiwan University, Taipei 10617, Taiwan, ROC
[b] Department of Mechanical Engineering, National Taiwan University of Science and Technology, Taipei 10660, Taiwan, ROC

ARTICLE INFO

Article history:
Received 26 September 2011
Accepted 1 December 2011
Available online 11 December 2011

Keywords:
D. Welding
E. Wear
F. Microstructure

ABSTRACT

Titanium nitrides (TiNs) powder was used as a material to resist wear; it was then clad onto a Ti–6Al–4V substrate by gas tungsten arc welding (GTAW). During the cladding process, the TiN_x reinforcing phase was formed *in situ* within the clad layer. Since the TiN_x reinforcing phase exists within the clad layer, the hardness of the clad layer is double that of the substrate. Wear test results reveal that the wear resistance of TiN clad layer is up to ten times more resistant than the Ti–6Al–4V substrate. From the worn surface analysis, the primary wear mechanism of the Ti–6Al–4V specimen exhibited oxidation wear combined with adhesive wear, and the TiN clad layer specimen exhibited abrasive wear. This investigation also discusses the mechanism for forming the clad layer microstructure. During solidification of the clad layer, the motion of the liquid–solid interface caused the oval TiN_x phase to cluster, producing a dendritic appearance.

1. Introduction

Titanium and its alloys are widely applied in aerospace, chemical, petrochemical and marine industries because of their prominent properties of high specific strength, excellent corrosion resistance and high temperature properties. Nevertheless, they are currently restricted to tribological applications, owing to their poor wear resistance (e.g. low adhesive and fretting wear resistance) and high galling tendency, both of which prevent them from being widely applied as engineering tribological components [1]. In order to improve the wear performance of pure titanium and its alloys, many technologies are being developed; surface treatment is one of the most efficient means. The common surface engineering methods include: ion implantation, laser cladding, thermal oxidation heat treatment, chemical vapor deposition, shielded metal arc welding and gas tungsten arc welding [2–5]. Gas tungsten arc welding (GTAW) is one of the most convenient methods of surface alloying and surface modification. GTAW can rapidly provide a thick and crack-free clad layer in all instances with metallurgical bonds at the interface between the clad layer and the substrate [6–8]. GTAW cladding also costs less than laser cladding. Furthermore, GTAW differs from the laser cladding in that it does not suffer from various coefficients of absorption of laser energy associated with a variety of powders [9]. The selection of the cladding powder is more flexible with the GTAW cladding.

Titanium nitrides (TiNs) have proven to be effective reinforcements of titanium and its alloys [10–12]. Their favorable properties include a high degree of hardness and excellent wear-resistance in numerous tribological systems [13]. Many studies have pointed out that the TiN dendrites possibly improve the titanium and its alloys wear properties [14], but few studies have explored the microstructure evolution.

Accordingly, in this investigation, the GTAW cladding method was applied to carry out the surface modification of an alloy. TiN powder was clad onto a Ti–6Al–4V alloy surface to improve its wear-resistance properties. The microstructural evolution is discussed, including that of reinforcements that were synthesized *in situ* within the TiN clad layer.

2. Experimental procedure

A Ti–6Al–4V alloy substrate was fabricated into a 19 mm × 20 mm × 100 mm cuboid specimen. The face which was to be clad was polished with sand paper to assure the quality of the clad surface. TiN powder was mixed with 4 wt.% polyvinyl alcohol and agitated to form a paste [15]. The paste was preplaced on the surface of the Ti–6Al–4V alloy substrate to a thickness of 2.0 mm. Finally, the specimen was put in a furnace and maintained at 60 °C for 24 h in order to remove moisture.

The GTAW was directed onto the specimen surface, as shown in Fig. 1. The parameters of the cladding process were set to a weld voltage $V = 17$ V, weld current $A = 120$ A (DC) and traveling speed $v = 0.65 \times 10^{-3}$ m/s.

* Corresponding author. Tel.: +886 2 2362 5489; fax: +886 2 3366 2699.
E-mail address: chen735@ntu.edu.tw (Y.-C. Chen).

0261-3069/$ - see front matter © 2011 Elsevier Ltd. All rights reserved.
doi:10.1016/j.matdes.2011.12.007

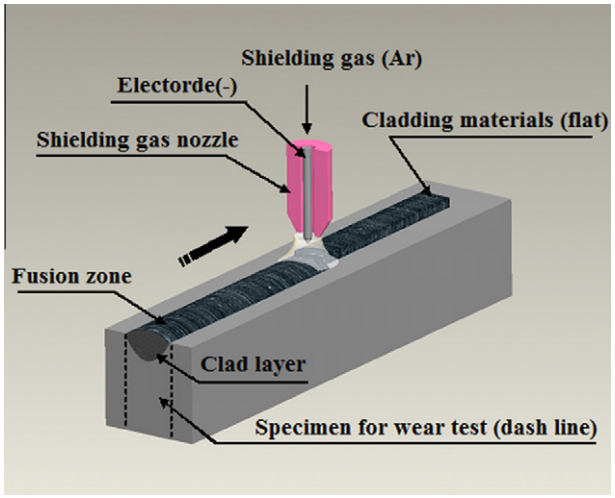

Fig. 1. Schematic illustration of the GTAW method.

After cladding, the cuboid was sectioned using a wire-EDM machine to prepare specimens for microstructural observation and wear testing. Metallographic specimens were prepared using a standard mechanical polishing process and then etched in a solution of Kroll's reagent to reveal the growth morphologies of the compounds within the clad layers. A field-emission scanning electron microscope (FESEM) and an electron probe microanalyzer (EPMA) were then used to observe the microstructure and analyze the compounds. The compounds and the phases of the clad layer were examined using an X-ray diffractometer (XRD).

The microhardness distribution profile of a cross-section of the clad layer was obtained using a Vickers microhardness tester at 1 kg loading with a loading time of 15 s. The tribological properties of the TiN clad layers and Ti–6Al–4V alloy specimens were explored using a pin-on-disk type rotating wear machine under dry sliding conditions at room temperature (see Fig. 2). A moving pin specimen was loaded and slid onto the flat surface of a stationary disk made of hardened AISI 52100 bearing steel which had a hardness of 62 HRC, diameter of 60 mm and a thickness of 8 mm. Prior to wear testing, the flat surface of the disk was polished to roughness Ra = 0.06 μm using up to 600 grit sand paper. Table 1 presents the wear test conditions.

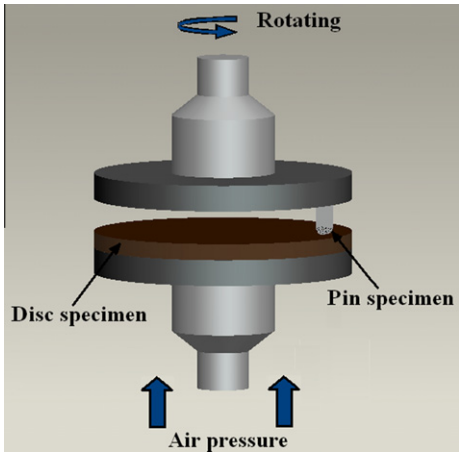

Fig. 2. Schematic illustration of the pin-on-disk wear test.

Table 1
The wear test conditions.

Sliding conditions	Dry sliding conditions
Load (N)	30
Sliding speed (m/s)	0.9
Sliding distance (m)	3257
Temperature (°C)	Room temperature

3. Results and discussion

3.1. Microstructural characteristics of titanium nitrides clad layers

The typical metallurgical micrographs of the cross-sections of different parts of the clad layer are presented in Fig. 3a–c. The microstructure of the clad layer reveals that oval particles and dendrites are dispersed uniformly within the matrix.

A comparison of Fig. 3a and b clearly reveals that reinforcements in the top layer are finer than those found in the middle of the clad layer. This difference may have been caused by different solidification rates in different regions of the same melting pool after cladding. During the cladding process, argon is blown onto the top of the melting pool, where the cooling rate and degree of supercooling exceed those found in the middle of the region; hence, the critical radius of nucleation is smaller and the number of nuclei is higher. Accordingly, reinforcements formed within the top layer are finer than those formed in the middle. Furthermore, the conduction of heat within the substrate can cause a high cooling rate at the bottom of the melting pool. Consequently, a high cooling rate causes the transformation of the heat-affected zone (HAZ) to martensite, as displayed in Fig. 3c.

To indicate the chemical composition and microstructures of the different phases, advanced examinations were performed. As presented in Figs. 4 and 5, the backscattered electron image (BEI) and quantitative analysis indicate that the oval or dendrite structures are rich in Ti and N elements. It can also be seen that the oval or dendrite structures were formed in two phases, indicated by A and B, respectively. In this result, the content of dark phase nitrogen atoms is higher than it is in the light phase. The XRD analysis reveals that TiN, $TiN_{0.3}$, $TiN_{0.26}$, α/martensite–Ti and β-Ti phase were present within the TiN clad layers, as displayed in Fig. 6. Similar phases, such as TiN, $TiN_{0.3}$ and $TiN_{0.26}$, have also been observed in previous laser cladding study [16]. These results verify that in the TiN clad layer, the reinforcement phases consist of both oval and dendrite TiN_x. Many researchers have pointed out that microstructure is a critical factor of improving clad layer properties. However, few studies have explored the microstructure evolution. So, if we can find the microstructure evolution mechanism, we can better understand the clad layer.

Based on the morphology and related analytical results of the microstructure of the TiN clad layer, the following hypothesis concerning evolution of this microstructure is proposed (Fig. 7). During cladding, a cuboid of TiN powder was preplaced on the substrate and then clad onto the substrate using GTAW. The cladding material and substrate were heated using an electrical arc (temp. ≒ 6000 °C), to produce a locally melted pool covered by the electrical arc on the cladding surface. The TiN particles were dissolved rapidly into the Ti and N atoms and distributed uniformly within the melted pool by thermal convection (Fig. 7a and b). The melting pool was cooled by the shielding gas and the conduction of heat through the substrate, initiating solidification as the arc moved. According to the Ti–N binary phase diagram [17], because the TiN particles dissolved and the substrate melted, the number of titanium atoms was enhanced while the number of nitrogen atoms was reduced. Therefore, during the solidification both the TiN and TiN_x phases were formed. During the β-Ti

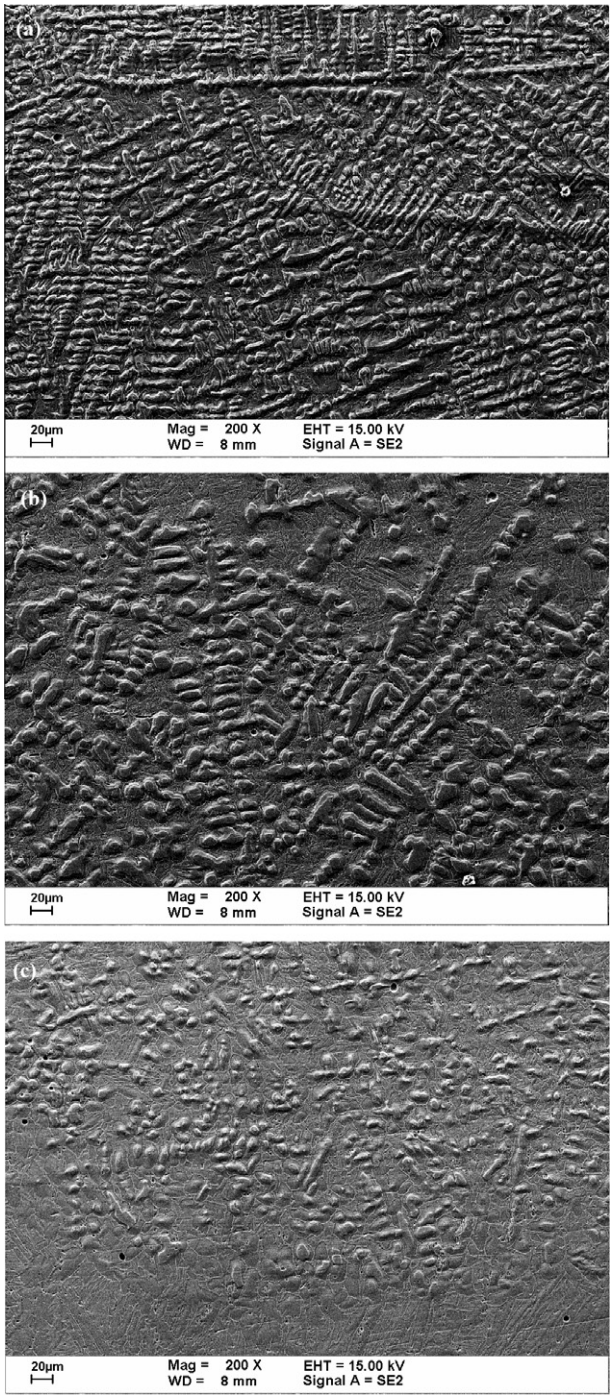

Fig. 3. SEM micrographs of (a) top region; (b) middle region; (c) bottom region and heat affected zone of TiN clad layer after etching in Kroll's regia for two hours.

solidification, oval TiN and TiN_x reinforcements were clustered by the push effect of the solid–liquid interfaces during matrix solidification (Fig. 7c). Then, TiN formed a dendritic morphology within the clad layer, as shown in Fig. 7d. Wu [18] also reported a similar push effect of the solid–liquid interfaces in a previous study. In that case, the TiC particles were uniformly distributed within interdendritic regions because of the push effect of the advancing solid–liquid interfaces. Martensite–Ti would also have formed due to the high rate of cooling within the matrix. The resulting matrix would therefore likely consist of a mixture of martensite–Ti and retained β-Ti.

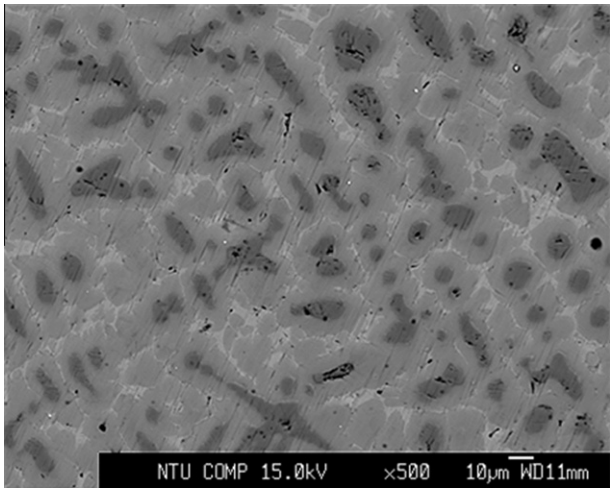

Fig. 4. Backscattered electron image of TiN clad layer.

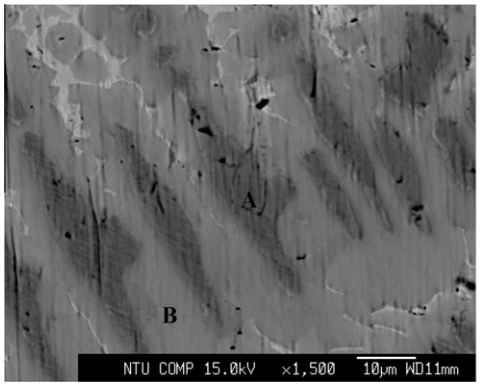

Caption A

Element	Atomic%
Ti	70.133
Al	0.672
V	0.563
N	28.632
Totals	100

Caption B

Element	Atomic%
Ti	78.094
Al	7.477
V	1.138
N	12.991
Totals	100

Fig. 5. Quantitative analysis of TiN dendrite.

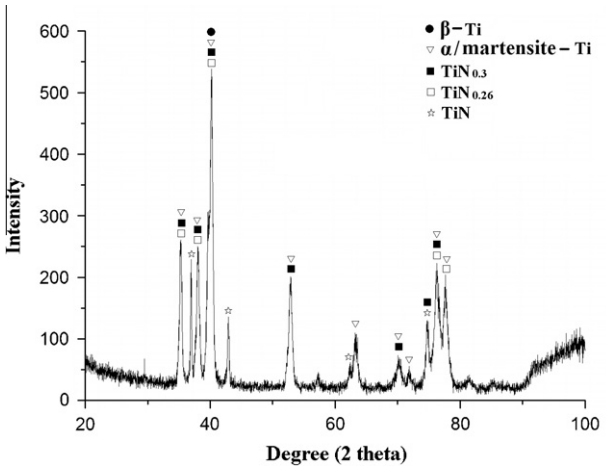

Fig. 6. X-ray diffraction spectra of TiN clad layer.

3.2. Wear behavior of titanium nitrides clad layers

Before the wear test was carried out, the hardness profile of the clad layer was evaluated by a Vickers Hardness tester. Fig. 8 shows the typical distribution of hardness through the clad layer cross-section. The maximum microhardness of the TiN clad layer reached

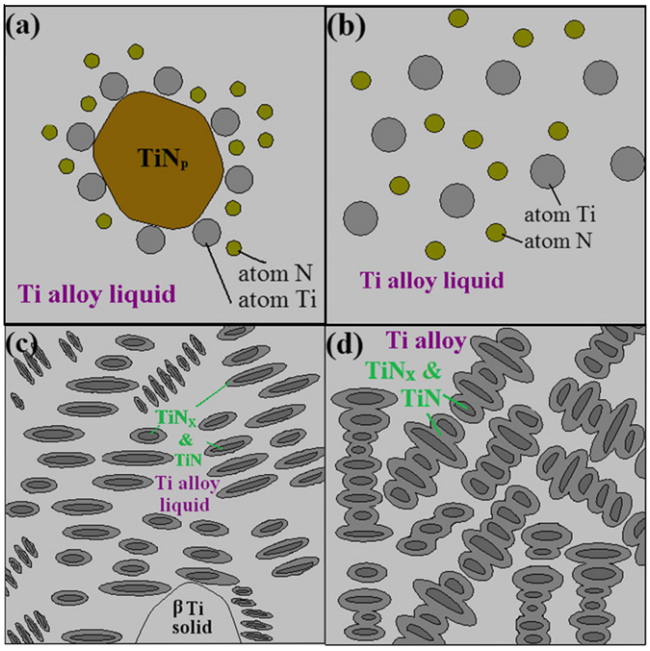

Fig. 7. The diagram illustration of microstructure how to form: (a) TiN particle surface partially melted; (b) TiN particles were melting quickly and the atoms of Ti and N were agitated and distributed in the melted pool uniformly; (c) the oval TiN_x reinforcement was clustered together by the push effect of the solid–liquid interfaces during matrix solidification; (d) oval TiN_x reinforcement pushing each other together then form a dendrite.

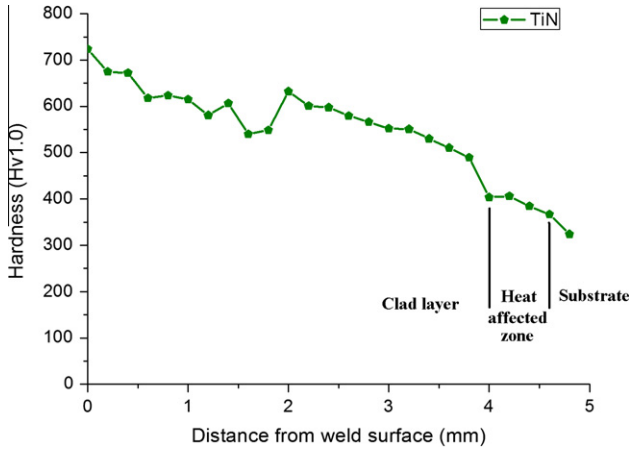

Fig. 8. Microhardness of the TiN clad layer.

approximately 740 $HV_{1.0}$, double that of the substrate (340 $HV_{1.0}$). Therefore, the precipitation strengthening of those reinforcements clearly improved the hardness of the clad layer. In addition, the microhardness of the clad layer gradually decreased with increase of distance from weld surface. The reason could be illustrated by the simple mixture rule. At top region, the distance between reinforcements is getting closer, so the deformation occurred mainly in reinforcements. On the other hand, with increase of distance from weld surface, the deformation occurred mainly in the matrix with little deformation of reinforcements [19]. Furthermore, the rapid heating and quenching effect strengthened the heat-affected zone (about 400 $HV_{1.0}$).

The wear performance of the TiN clad and Ti–6Al–4V specimens was evaluated under dry sliding wear test conditions. Fig. 9 plots

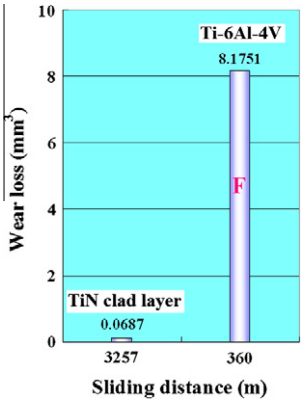

Fig. 9. Wear volume loss (c.f.: F = failure).

the loss of volume due to wear for the Ti–6Al–4V and the TiN clad specimens after sliding 3257 m at a sliding speed of 0.9 m/s. In this study, the Ti–6Al–4V specimen appeared worn after a sliding distance of approximately 360 m. In contrast, the TiN clad layer specimen slid about ten times distance, but the wear loss was only 0.84% of that of the failed Ti–6Al–4V specimen. Hence, TiN clad layer markedly improved the wear resistance of the substrate.

Fig. 10 presents evidence that the average friction coefficient for the TiN clad layer specimen was a little higher than that of the Ti–6Al–4V specimen. During the sliding wear test, the reinforcement of the TiN clad layer was responsible for the two-body abrasive wear, which increased the frictional force. However, as the temperature of the Ti–6Al–4V specimen surface increased, thick oxide films were produced, causing the friction coefficient to be lower than that of the TiN clad layer specimen. Furthermore, the friction coefficient for the TiN clad layer had large vibration amplitude with increasing distance. It was because the reinforcements were pulled out, and the wear mechanism was from two-body abrasive wear transformed into three-body abrasive wear.

Figs. 11 and 12 show the worn surfaces of the Ti–6Al–4V and the TiN clad layer specimens. The worn surface of the TiN clad layer specimen exhibited some abrasive wear and smooth surface pits, but the Ti–6Al–4V specimen exhibited oxidation wear combined with adhesive wear. When the sliding surfaces were subjected to loading and contact with each other, the asperities of the thick oxide films with the lower yield strength easily caused plastic deformation. Accordingly, the cold welding during plastic

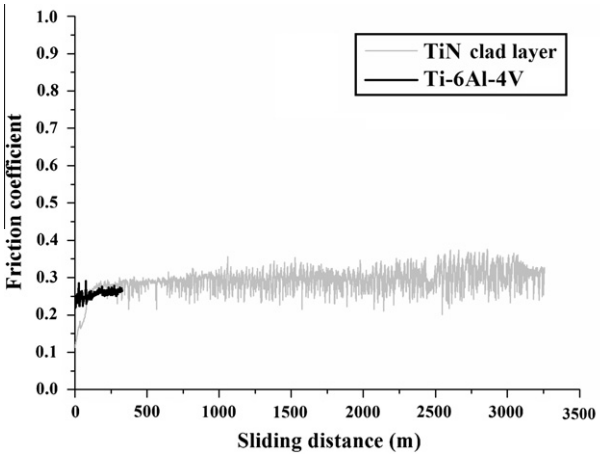

Fig. 10. The friction coefficient as a function of sliding distance.

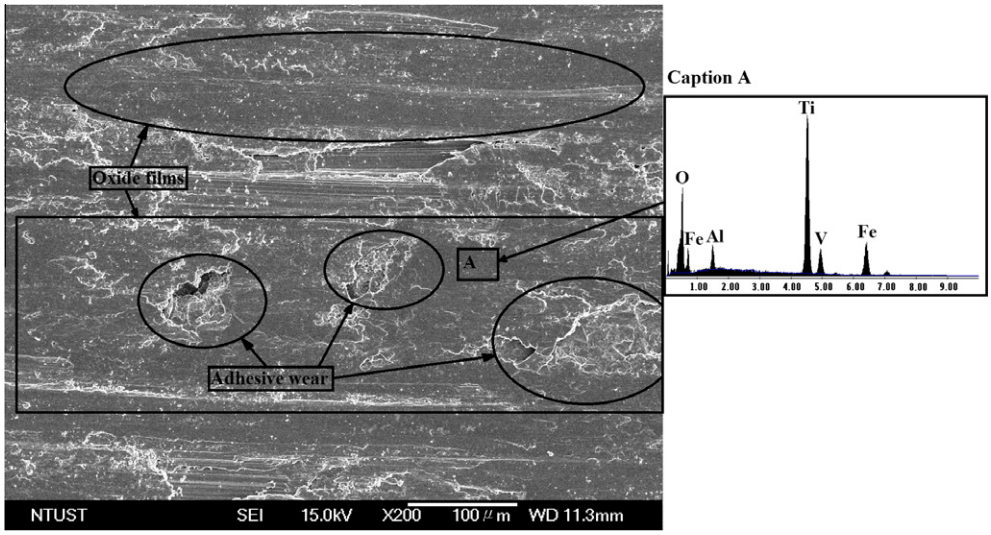

Fig. 11. Typical worn surface of the Ti–6Al–4V specimen. (caption A: EDS analysis of the oxide film).

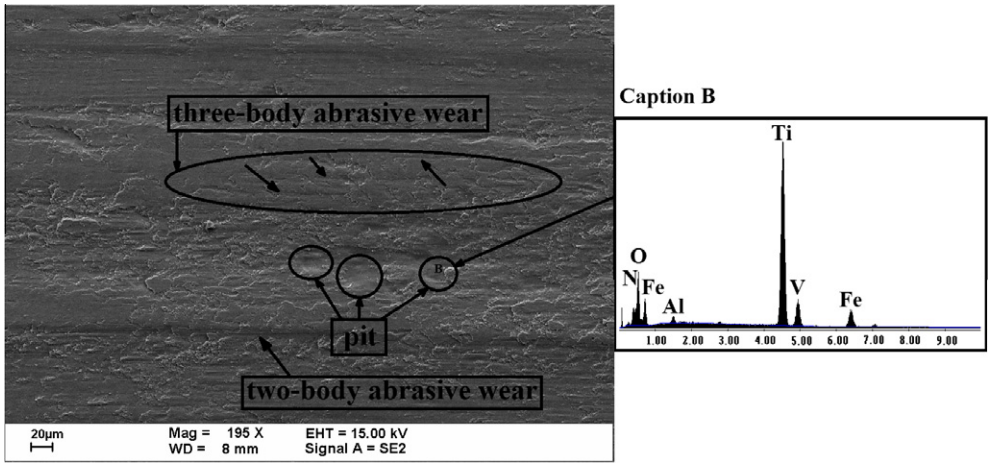

Fig. 12. Typical worn surface of the TiN clad layer specimen (caption B: EDS analysis of the smooth surface pit).

deformation formed junctions between the asperities that were in contact with each other. During sliding, the junctions were subjected to shearing, which may have broken the junctions and formed uneven surfaces, resulting in notable adhesive wear, as shown in Fig. 11. Some poor wear characteristics, such as serious adhesive wear and oxidation wear, of the Ti–6Al–4V worn surfaces were also observed in the other study, irrespective of the sliding velocity and applied load [20]. However, the TiN clad specimen exhibited excellent wear resistance properties for adhesion during sliding. As shown in Fig. 12, there was an absence of the morphological characteristics of adhesive wear on the worn surface. The excellent wear performance of the TiN clad layer was related to its reinforcements, whereas the very high hardness of TiN_x reinforcements made it very difficult for the clad layer to experience serious adhesion and plastic deformation. During sliding, the reinforcement of the TiN clad layer was responsible for the two-body abrasive wear. However, with increasing distance, the matrix was scraped, some oval TiN and TiN_x reinforcements would be pulled out from TiN clad layer and formed some smooth surface pits. Then these hard reinforcements probably caused the three-body abrasive wear. But the complex shape such as the dendrite structure was not pulled out easily and could effectively prevent the matrix from exhibiting plastic flow. So the worn surface was characterized by the presence of more abrasive wear features than in the Ti–6Al–4V specimen.

The TiN clad layer of Ti–6Al–4V exhibited excellent wear resistance of abrasion and adhesion under sliding conditions because of the TiN_x reinforcements formed *in situ* which markedly increased the strength and hardness of the clad layer.

4. Conclusions

The experimental results associated with the microstructural analysis and the wear test support the following conclusions. TiN_x reinforcements were successfully produced by an *in situ* reaction during the GTAW process and were uniformly dispersed within the TiN clad layer. During solidification, the motion of the liquid–solid interface caused the oval TiN_x phase to cluster, producing a dendritic appearance. Those TiN_x reinforcements clearly enhanced the wear resistance of the clad layer. The main wear mechanism of the TiN clad layer specimen exhibited abrasive wear, and the Ti–6Al–4V specimen exhibited oxidation wear combined with adhesive wear.

Acknowledgement

The authors would like to thank the National Science Council of the Republic of China, Taiwan, for financially supporting this research under Contract No. NSC100-2221-E-002-047-MY3.

References

[1] Bell T. Proceedings of the first Asian international conference on tribology. Beijing: Tsinghua University Press; 1998. p. 421.
[2] Muthukumaran V, Selladurai V, Nandhakumar S, Senthilkumar M. Experimental investigation on corrosion and hardness of ion implanted AISI 316L stainless steel. Mater Des 2011;31:2813–7.
[3] Borgioli F, Galvanetto E, Iozzelli F, Pradelli G. Improvement of wear resistance of Ti–6Al–4V alloy by means of thermal oxidation. Mater Lett 2005;59:2159–62.
[4] Tian YS, Chen CZ, Chen LX, Huo QH. Microstructures and wear properties of composite coatings produced by laser alloying of Ti–6Al–4V with graphite and silicon mixed powders. Mater Lett 2006;60:109–13.
[5] Shamanian M, Mousavi Abarghouie SMR, Mousavi Pour SR. Effects of surface alloying on microstructure and wear behavior of ductile iron. Mater Des 2010;31:2760–6.
[6] Arabi Jeshvaghani R, Shamanian M, Jaberzadeh M. Enhancement of wear resistance of ductile iron surface alloyed by stellite 6. Mater Des 2011;32:2028–33.
[7] Lin YC, Wang SW, Wu KE. The wear behaviour of machine tool guideways clad with W–Ni, W–Co and W–Cu using gas tungsten arc welding. Surf Coat Technol 2003;172:158–65.
[8] Lin Yuan Ching, Wang Shi Wei, Lin Yu Chang. Analysis of microstructure and wear performance of WC–Ti clad layers on steel, produced by gas tungsten arc welding. Surf Coat Technol 2005;200:2106–13.
[9] Cai Lifang, Zhang Yongzhong, Shi Likai. Microstructure and formation mechanism of titanium matrix composites coating on Ti–6Al–4V by laser cladding. Rare Metals 2007;26:342–6.
[10] Khan TI, Fowles D. The surface modification of a Ti–6Al–4V alloy using a metal arc heat source. In: Sudershan TS, Khor KA, Jeandin M, editors. Surface modification technologies X. The Institute of Materials; 1997. p. 469–77.
[11] Nunogaki M. Transformation of titanium surface to TiC- or TiN-ceramics by reactive plasma processing. Mater Des 2001;22:601–4.
[12] Hu Rui Hua, Lim Jae Kyoo. Hardness and wear resistance improvement of surface composite layer on Ti–6Al–4V substrate fabricated by powder sintering. Mater Des 2010;31:2670–5.
[13] Duverneix T, Puig T, Bataille F. ICALEO'90: Laser Materials Processing. In: Ream SL, Dausinger F, Fujioka T, editors. SPIE; 1991. p. 525.
[14] Jiang P, He XL, Li XX, Yu LG, Wang HM. Wear resistance of a laser surface alloyed Ti–6Al–4V alloy. Surf Coat Technol 2000;130:24–8.
[15] Lin YC, Cho YH. Elucidating the microstructure and wear behavior for multicomponent alloy clad layers by in situ synthesis. Surf Coat Technol 2008;202:4666–72.
[16] Tina YS, Chen CZ, Chen LX, Huo QH. Crack-free wear resistance coatings produced on pure titanium and Ti–6Al–4V by laser nitriding. Surf Rev Lett 2005;12:741–4.
[17] ASM. Metals Handbook, vol. 3. 8th ed. Alloy Phase Diagrams. ASM International; 1992.
[18] Wu X. In situ formation by laser cladding of a TiC composite coating with a gradient distribution. Surf Coat Technol 1999;115:111–5.
[19] Kim HS. On the rule of mixtures for the hardness of particle reinforced composites. Mater Sci Eng A 2000;289:30–3.
[20] Straffelini G, Molinari A. Dry sliding wear of Ti–6Al–4V alloy as influenced by the counterface and sliding conditions. Wear 1999;236:328–38.